Coherent propagation and optical pumping in three-level systems

Bruce J. Herman, Peter D. Drummond,* J. H. Eberly, and B. Sobolewska†
Department of Physics and Astronomy, University of Rochester, Rochester, New York 14627
(Received 2 February 1984)

We develop a theory to take into account the effects in coherent propagation of a small overlapping of the pump and probe pulses in a three-level system. The Maxwell equations reduce to coupled equations for variables which are related to the time-integrated field envelopes. We make comparisons of the propagation results to the Burnham-Chiao theory for a two-level amplifier and can predict when this theory breaks down. An application to superfluorescence is presented where a lengthening of the delay time is found. We treat Doppler broadening and find simplified equations in two cases: (a) a very broad line and (b) a very narrow line where the initial and final states are degenerate. For the broad-line case, with an appropriate choice of initial parameters, we can make the probe pulse approach any desired area for certain configurations of the levels.

I. INTRODUCTION

There are many situations in quantum optics where one deals with three-level systems, for example, Raman amplifiers, simultons, and superfluorescence. Some of these, particularly amplifiers and superfluorescence, have been treated in the past with the use of two-level models[1–11] which ignore the pumping process that inverts the population in the system. Since this pumping is inherently part of the dynamics of the system, it can have profound effects on the system's evolution. Two-level models cannot take these effects into account.

One method of inverting the system is to use a laser pulse resonant with the pumping transition frequency. A treatment of coherent resonant propagation for nonoverlapping pulses in a Raman amplifier has been given by Sobolewska *et al.*[12] This paper is an expansion and extension of that work. (Exact solutions for some propagation problems in three-level systems have also recently been found.[13–16]) Here we treat all configurations for a three-level system. Population is pumped from the first to the second level by an input pulse. Then the second-to-third level transition is investigated by injecting a probe pulse. In the ideal case the pump and probe pulses are completely separated in time. Thus the probe pulse will only interact with the population transferred by the pump. In actuality, however, the pump pulse changes in time due to propagation and the two pulses will not remain completely nonoverlapping. In this paper we develop a theory to take into account the effects of a small overlap between the propagating pulses.

In Sec. II the notation and the atomic equations of motion on resonance are defined. In Sec. III approximations are used in order to solve for the time development of the atomic system. The expressions obtained for the dipoles are incorporated into the Maxwell equations in Sec. IV where the "partial area" equations are derived. Numerical solutions of the partial area equations are compared and contrasted to the exact solutions and to a two-level theory in Sec. V. An application of the theory to a calculation of the delay time in superfluorescence is given in Sec. VI. Section VII treats Doppler broadening. We summarize our results in Sec. VIII.

II. RESONANT ATOMIC EQUATIONS OF MOTION

We will concern ourselves only with plane-wave propagation of electromagnetic radiation in an atomic or molecular medium with three energy levels. The levels are numbered so that levels 1 and 2 are dipole coupled as are levels 2 and 3; however, transitions between levels 1 and 3 are forbidden. Levels 1, 2, and 3 are defined to have energies $\hbar\omega_1$, $\hbar\omega_2$, and $\hbar\omega_3$, respectively.

The levels can be arranged in three distinct ways according to the relationships among the energies of the levels: Λ, V, and cascade. We take the cascade to have two variations according to whether $\omega_1 > \omega_2$ or $\omega_1 < \omega_2$. These are called cascade A and cascade B, respectively. The configurations for the different cases are shown in Fig. 1.

We will only treat systems whose homogeneous decay times are much longer than the input radiation pulse lengths. Thus we can neglect decay mechanisms such as collisional broadening or radiative decay and deal ex-

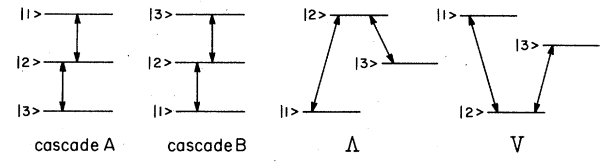

FIG. 1. The different level configurations treated in this paper. Level $|2\rangle$ is always dipole coupled to levels $|1\rangle$ and $|3\rangle$. Transitions between levels $|1\rangle$ and $|3\rangle$ are forbidden. We make the distinction of two arrangements for the cascade configuration depending upon whether the energy of level $|1\rangle$ is greater (cascade A) or less than (cascade B) the energy of level $|2\rangle$. We do this since we will always take the initial population to be in level $|1\rangle$. Thus cascade A is an amplifier while cascade B is an absorber.

clusively with coherent propagation. Under these conditions the interaction picture will be used, since this will allow for us a simple interpretation of the results. Inhomogeneous broadening will be treated in Sec. VII.

We will denote the atomic states with energies $\hbar\omega_1$, $\hbar\omega_2$, and $\hbar\omega_3$ by $|1\rangle$, $|2\rangle$, and $|3\rangle$, respectively. During the time scales of interest we will assume these states form an orthonormal complete set, with the state $|1\rangle$ initially occupied.

We will use the dipole and semiclassical approximations[17] and treat the electric field $\vec{E}$ as a classical variable. The Hamiltonian of each atom is given by

$$\hat{H}_A=\hat{H}_0+\hat{H}_I=\sum_{j=1}^{3}\hbar\omega_j\hat{\sigma}_{jj}-\hat{\vec{d}}\cdot\vec{E}$$
$$=\sum_{j=1}^{3}\hbar\omega_j\hat{\sigma}_{jj}-[(\vec{d}_{12}\hat{\sigma}_{12}+\vec{d}_{23}\hat{\sigma}_{23})+\text{H.c.}]\cdot\vec{E}\ , \tag{2.1}$$

where the $\hat{\sigma}_{jk}=|j\rangle\langle k|$ are the atomic projection operators and $\hat{\vec{d}}=\sum_{j,k}\vec{d}_{jk}\hat{\sigma}_{jk}$ is the dipole moment. In the interaction picture, the evolution operator obeys the Schrödinger equation

$$i\hbar\frac{\partial}{\partial t}\hat{U}_I=\hat{V}_I\hat{U}_I\ , \tag{2.2}$$

where

$$\hat{V}_I=\hat{U}_0^{\dagger}\hat{H}_I\hat{U}_0,\quad \hat{U}_0=\exp\left[\frac{1}{i\hbar}\hat{H}_0t\right]. \tag{2.3}$$

For an electric field propagating in the z direction, if $\vec{E}$ has components oscillating only near frequencies ω and ω' we may write

$$\vec{E}=\{\vec{\epsilon}_1\mathscr{E}_1\exp[-is_1(\omega t-kz)]$$
$$+\vec{\epsilon}_2\mathscr{E}_2\exp[-is_2(\omega' t-k'z)]\}+\text{c.c.}\ , \tag{2.4}$$

where $k=\omega/c$, $k'=\omega'/c$, and $\mathscr{E}_j=\mathscr{E}_j(t,z)$ is the jth pulse's amplitude which is taken to vary slowly in an optical cycle. s_j is defined to be the sign of the energy difference $\hbar(\omega_{j+1}-\omega_j)=\hbar\omega_{j+1,j}$. We will choose the fields $\mathscr{E}_1$ and $\mathscr{E}_2$ to be tuned on resonance with the $1\leftrightarrow2$ and $2\leftrightarrow3$ transitions, respectively, by taking $\omega=|\omega_{21}|$ and $\omega'=|\omega_{32}|$. Then, combining Eqs. (2.1), (2.3), and (2.4) and using the rotating-wave approximation[18] (RWA) we obtain

$$\hat{V}_I=\frac{i\hbar}{2}[(\Omega_1\hat{\sigma}_{21}+\Omega_2\hat{\sigma}_{32})-\text{H.c.}]\ , \tag{2.5a}$$

where the Rabi frequencies, chosen to be real, are defined with an "extra" factor of $-i$ for convenience:

$$\Omega_1=\frac{2\vec{d}_{21}\cdot\vec{\epsilon}_1\mathscr{E}_1}{i\hbar},\quad \Omega_2=\frac{2\vec{d}_{32}\cdot\vec{\epsilon}_2\mathscr{E}_2}{i\hbar}\ . \tag{2.5b}$$

The solution for the interaction evolution operator is then given by the time-ordered expression

$$\hat{U}_I(t)=P\exp\left[\frac{1}{i\hbar}\int_0^t\hat{V}_I(t')dt'\right], \tag{2.6}$$

where P is the Dyson time-ordering operator.[19] Now we may write

$$\hat{U}_I(t)=P\exp[-i\hat{l}_1\theta_2(t)-i\hat{l}_3\theta_1(t)]\ , \tag{2.7a}$$

where

$$\theta_j(t)=\int_0^t\frac{\Omega_j(t')}{2}dt',\quad j=1,2 \tag{2.7b}$$

$$\hat{l}_3=i(\hat{\sigma}_{21}-\hat{\sigma}_{12})\ , \tag{2.7c}$$

$$\hat{l}_1=i(\hat{\sigma}_{32}-\hat{\sigma}_{23})\ . \tag{2.7d}$$

If we also define

$$\hat{l}_2=i(\hat{\sigma}_{13}-\hat{\sigma}_{31}) \tag{2.7e}$$

then

$$[\hat{l}_j,\hat{l}_k]=i\hat{l}_m,\quad j,k,m=1,2,3;2,3,1;3,1,2 \tag{2.8}$$

that is, $\hat{l}_1$, $\hat{l}_2$, and $\hat{l}_3$ are angular momentum operators.

These angular momentum operators are the generators of infinitesimal rotations and thus $\hat{U}_I(t)$ is a (time-ordered) rotation operator in a three-dimensional space spanned by $\{|1\rangle, |2\rangle, |3\rangle\}$.

It is easy to verify that the operator $e^{-i\phi\hat{l}_j}$ will rotate a vector $|\psi\rangle$ through an angle ϕ about the $|j\rangle$ axis. The extra factor of $-i$ is used in (2.5b) because it leads to rotations with real angles. We will use this information in Sec. III to develop approximate solutions for the effect of the evolution operator on a given initial state for the case of small overlap of the pulses Ω_1 and Ω_2.

III. APPROXIMATIONS FOR TIME DEVELOPMENT

Since there are no losses from the system, the length of the state vector $|\psi\rangle$ will remain constant throughout the propagation and retain its initial value of $\sqrt{\langle\psi|\psi\rangle}=1$. Thus, from Sec. II, the effect of the operator $\hat{U}_I(t)$ on the initial state $|\psi\rangle$ will be to rotate the vector $|\psi\rangle$ to some point on the unit sphere. It is also possible to reach the same point by performing two successive rotations on $|\psi\rangle$ about two orthogonal axes through two different angles. [This is merely a consequence of the fact that the angular momentum operators form a Lie algebra. We can then find coefficients $b_i(t)$ such that we may write $\exp(a_1\hat{l}_1+a_2\hat{l}_2+a_3\hat{l}_3)=\exp(b_1\hat{l}_1)\exp(b_2\hat{l}_2)\exp(b_3\hat{l}_3)$ for any coefficients $a_i(t)$.[20]] For example, if $|\psi\rangle$ is initially the state $|1\rangle$, then any point on the unit sphere can be reached by first rotating about the $|3\rangle$ axis and then about the $|1\rangle$ axis. Specifically, there exist angles ϕ_1 and ϕ_2 such that

$$|\psi(t)\rangle=\sum_{j=1}^{3}\psi_j(t)|j\rangle=\hat{U}_I(t)|1\rangle$$
$$=e^{-i\phi_2\hat{l}_1}e^{-i\phi_1\hat{l}_3}|1\rangle \tag{3.1}$$

(see Fig. 2). If $|\psi(t)\rangle$ is expanded on the basis set $\{|1\rangle, |2\rangle, |3\rangle\}$, this can be written as the matrix equation

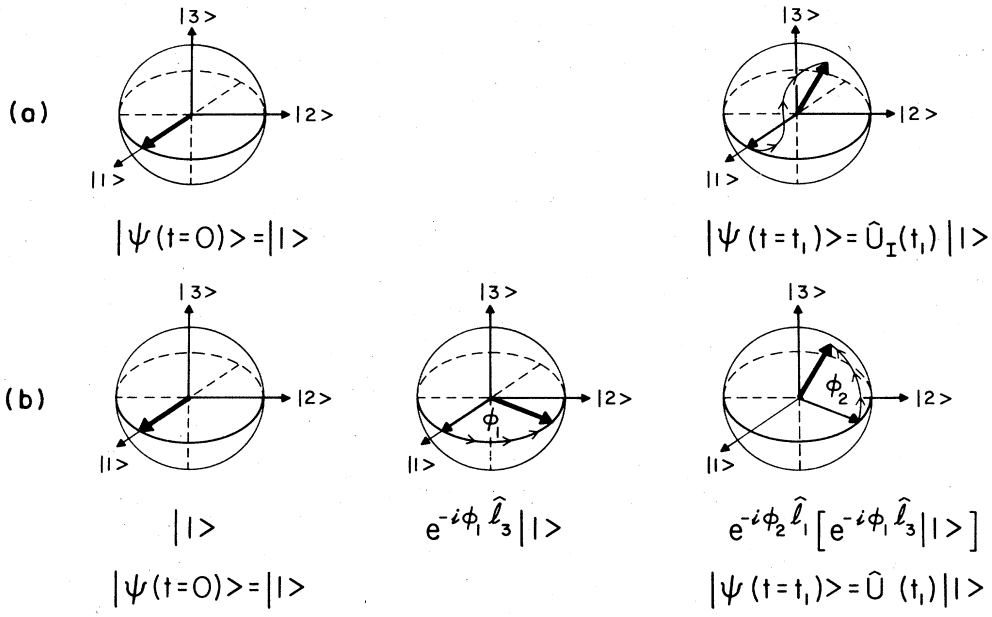

FIG. 2. Time development of the state vector $|\psi\rangle$. (a) $|\psi\rangle$ evolves under the action of the time evolution operator $\hat{U}_I$ going initially from $|\psi\rangle=|1\rangle$ at time $t=0$ to $|\psi\rangle=\hat{U}_I(t_1)|1\rangle$ at time $t=t_1$. Tip of the state vector traces out a path on the surface of the unit sphere. (b) We can have $|\psi\rangle$ reach the same point of the unit sphere at time t_1 by first rotating about the $|3\rangle$ axis through an angle ϕ_1 and then about the $|1\rangle$ axis through an angle ϕ_2. ϕ_1 and ϕ_2 are just the polar and azimuthal angles, respectively, of the state vector with reference to $|1\rangle$ as the polar axis.

$$\begin{bmatrix}\psi_1(t)\\ \psi_2(t)\\ \psi_3(t)\end{bmatrix}=\begin{bmatrix}1 & 0 & 0\\ 0 & \cos\phi_2 & -\sin\phi_2\\ 0 & \sin\phi_2 & \cos\phi_2\end{bmatrix}\begin{bmatrix}\cos\phi_1 & -\sin\phi_1 & 0\\ \sin\phi_1 & \cos\phi_1 & 0\\ 0 & 0 & 1\end{bmatrix}\begin{bmatrix}1\\ 0\\ 0\end{bmatrix}. \tag{3.2}$$

We therefore obtain the following set of equations relating the ψ's to the ϕ's:

$$\psi_1(t)=\cos\phi_1(t)\,, \tag{3.3a}$$

$$\psi_2(t)=\cos\phi_2(t)\sin\phi_1(t)\,, \tag{3.3b}$$

$$\psi_3(t)=\sin\phi_2(t)\sin\phi_1(t)\,. \tag{3.3c}$$

Thus ϕ_1 and ϕ_2 are just the polar and azimuthal angles, respectively, of the state vector $|\psi\rangle$, taking $|1\rangle$ as the polar axis.

Now, $|\psi(t)\rangle$ also obeys the Schrödinger equation generated by the Hamiltonian Eq. (2.5), and using Eq. (3.1) we derive for the ψ's

$$\frac{\partial}{\partial t}\psi_1(t)=-\frac{\Omega_1}{2}\psi_2(t)\,, \tag{3.4a}$$

$$\frac{\partial}{\partial t}\psi_2(t)=\frac{\Omega_1}{2}\psi_1(t)-\frac{\Omega_2}{2}\psi_3(t)\,, \tag{3.4b}$$

$$\frac{\partial}{\partial t}\psi_3(t)=\frac{\Omega_2}{2}\psi_2(t)\,. \tag{3.4c}$$

Hence from Eqs. (3.3) and (3.4)

$$\frac{\partial}{\partial t}(\cos\phi_1)=-\frac{\Omega_1}{2}\cos\phi_2\sin\phi_1\,, \tag{3.5a}$$

$$\frac{\partial}{\partial t}(\cos\phi_2\sin\phi_1)=\frac{\Omega_1}{2}\cos\phi_1-\frac{\Omega_2}{2}\sin\phi_2\sin\phi_1\,, \tag{3.5b}$$

$$\frac{\partial}{\partial t}(\sin\phi_2\sin\phi_1)=\frac{\Omega_2}{2}\cos\phi_2\sin\phi_1\,. \tag{3.5c}$$

We may integrate Eqs. (3.5a) and (3.5c) to obtain the implicit solutions

$$\phi_1(t)=\int_0^t\frac{\Omega_1(t')}{2}\cos\phi_2(t')dt'\,, \tag{3.6a}$$

$$\sin\phi_2(t)=\csc\phi_1(t)\int_0^t\frac{\Omega_2(t')}{2}\cos\phi_2(t')\sin\phi_1(t')dt'\,. \tag{3.6b}$$

These equations are exact. We see from Fig. 2(b) that when ϕ_2 is a small angle, ψ_3 will also be small and thus the induced polarization in the second transition, proportional to $\psi_2\psi_3$, will have a small magnitude. Since ϕ_2 becomes nonzero only after Ω_2 arrives we see that we can describe the beginning of the amplification (or absorption) process in the second transition by taking $|\phi_2|\ll 1$. Under this approximation we can set $\cos\phi_2\simeq 1$ and $\sin\phi_2\simeq\phi_2$ and then Eqs. (3.6) become

$$\phi_1(t)=\int_0^t\frac{\Omega_1(t')}{2}dt'\,, \tag{3.7a}$$

$$\phi_2(t)=\csc\phi_1(t)\int_0^t\frac{\Omega_2(t')}{2}\sin\phi_1(t')dt' \tag{3.7b}$$

and for consistency we require

$$\left|\csc\phi_1(t)\int_0^t\frac{\Omega_2(t')}{2}\sin\phi_1(t')dt'\right|\ll 1\ ,$$

or

$$\left|\int_0^t\frac{\Omega_2(t')}{2}\sin\phi_1(t')dt'\right|\ll|\sin\phi_1(t)|\leq 1\ . \tag{3.8}$$

However, it is obvious that

$$\left|\int_0^t\frac{\Omega_2(t')}{2}\sin\phi_1(t')\right|dt'\leq\int_0^t\left|\frac{\Omega_2(t')}{2}\right|dt'\ . \tag{3.9}$$

Thus a sufficient condition for the relations (3.7) to hold is

$$\int_0^t\left|\frac{\Omega_2(t')}{2}\right|dt'\ll 1\ , \tag{3.10}$$

i.e., the integrated magnitude of the second pulse envelope is required to remain small.[21]

We can relax our requirement of small ϕ_2, thus allowing for an arbitrary polarization in the second transition, as follows. When the pulses are completely nonoverlapping, i.e., when there exists a time t_0 such that $\Omega_1(t\geq t_0)=0$ and $\Omega_2(t\leq t_0)=0$, then Eqs. (3.6) reduce to the quantum-mechanical pulse areas. Let us assume that the pulses overlap until a time t_0 after which $\Omega_1(t)=0$,[22] and that during the overlap, $\int_0^t|\Omega_2(t')/2|dt'\ll 1$. When these conditions hold we will say that the pulses have small overlap. For times $t\leq t_0$, the angles $\phi_1(t)$ and $\phi_2(t)$ are given by Eqs. (3.7) while for times $t\geq t_0$ we have

$$\phi_1(t)=\phi_1(t_0)+\int_{t_0}^t\frac{\Omega_1(t')}{2}dt'\ , \tag{3.11a}$$

$$\phi_2(t)=\phi_2(t_0)+\int_{t_0}^t\frac{\Omega_2(t')}{2}dt'\ . \tag{3.11b}$$

Hence Eq. (3.11a) is identical in form to Eq. (3.7a) while Eq. (3.11b) can be written as

$$\begin{aligned}\phi_2(t\geq t_0)&=\phi_2(t_0)+\csc\phi_1(t_0)\int_{t_0}^t\frac{\Omega_2(t')}{2}\sin\phi_1(t_0)dt'\\&=\phi_2(t_0)+\csc\phi_1(t)\int_{t_0}^t\frac{\Omega_2(t')}{2}\sin\phi_1(t')dt'\\&=\csc\phi_1(t)\int_0^t\frac{\Omega_2(t')}{2}\sin\phi_1(t')dt'\end{aligned} \tag{3.12}$$

since $\phi_1(t\geq t_0)=\phi_1(t_0)$. Thus for the case of small overlap of the pulses, the solutions (3.7) are valid even for large ϕ_2. Since we now have an approximate expression for the time development of the system when it starts in the state $|1\rangle$, we may compute the polarization of the medium in terms of the derived angles ϕ_1 and ϕ_2 in order to calculate the effects on the propagating fields.

IV. PARTIAL AREA EQUATIONS

The reduced Maxwell equations for the fields Ω_1 and Ω_2 are easily derived under the slowly varying envelope approximation (SVEA).[23] We find

$$\frac{\partial}{\partial z}\Omega_1=-s_1\kappa_1\langle\hat{\sigma}_{12}\rangle\ , \tag{4.1a}$$

$$\frac{\partial}{\partial z}\Omega_2=-s_2\kappa_2\langle\hat{\sigma}_{23}\rangle\ , \tag{4.1b}$$

where

$$\kappa_1=\frac{\mathcal{N}|\vec{d}_{21}\cdot\vec{\epsilon}_1|^2|\omega|}{\epsilon_0\hbar c},\quad \kappa_2=\frac{\mathcal{N}|\vec{d}_{32}\cdot\vec{\epsilon}_2|^2|\omega'|}{\epsilon_0\hbar c}\ , \tag{4.1c}$$

and $\mathcal{N}$ is the number density of atoms (or molecules) in the medium. We have transformed to the moving frame by the relations

$$z=\mathfrak{z},\quad \tau=t-\mathfrak{z}/c\ . \tag{4.2}$$

Since we are taking the system to start in the state $|1\rangle$, $|\psi\rangle$ is given by Eqs. (3.3):

$$\begin{aligned}|\psi(\tau)\rangle=&\cos\phi_1(\tau)|1\rangle+\cos\phi_2(\tau)\sin\phi_1(\tau)|2\rangle\\&+\sin\phi_2(\tau)\sin\phi_1(\tau)|3\rangle\ .\end{aligned} \tag{4.3}$$

Thus

$$\begin{aligned}\langle\hat{\sigma}_{12}\rangle&=\langle\psi|1\rangle\langle 2|\psi\rangle=\cos\phi_1\cos\phi_2\sin\phi_1\\&=\tfrac{1}{2}\sin(2\phi_1)\cos\phi_2\ ,\end{aligned} \tag{4.4a}$$

$$\begin{aligned}\langle\hat{\sigma}_{23}\rangle&=\langle\psi|2\rangle\langle 3|\psi\rangle=\sin^2\phi_1\cos\phi_2\sin\phi_2\\&=\tfrac{1}{2}\sin^2\phi_1\sin(2\phi_2)\ .\end{aligned} \tag{4.4b}$$

Using the small-overlap approximation Eqs. (3.7), which we can write as

$$\Omega_1(\tau)=2\frac{\partial}{\partial\tau}\phi_1(\tau)\ , \tag{4.5a}$$

$$\Omega_2(\tau)=2\csc\phi_1(\tau)\frac{\partial}{\partial\tau}[\phi_2(\tau)\sin\phi_1(\tau)]\ , \tag{4.5b}$$

and combining these with Eqs. (4.1) and (4.4) gives us

$$\frac{\partial^2}{\partial z\partial\tau}\phi_1=-s_1\frac{\kappa_1}{4}\sin(2\phi_1)\cos\phi_2\ , \tag{4.6a}$$

$$\frac{\partial}{\partial z}\left[\csc\phi_1\frac{\partial}{\partial\tau}(\phi_2\sin\phi_1)\right]=-s_2\frac{\kappa_2}{4}\sin^2\phi_1\sin(2\phi_2)\ . \tag{4.6b}$$

If we define "areas" A_1 and A_2 such that

$$A_1=2\phi_1,\quad A_2=2\phi_2\ , \tag{4.7}$$

then Eqs. (4.6) become the partial area equations

$$\frac{\partial^2}{\partial z\partial\tau}A_1=-s_1\frac{\kappa_1}{2}\sin A_1\cos\left[\frac{A_2}{2}\right]\ , \tag{4.8a}$$

$$\begin{aligned}&\frac{\partial}{\partial z}\left[\csc\left[\frac{A_1}{2}\right]\frac{\partial}{\partial\tau}A_2\sin\left[\frac{A_1}{2}\right]\right]\\&\qquad=-s_2\frac{\kappa_2}{2}\sin^2\left[\frac{A_1}{2}\right]\sin A_2\ .\end{aligned} \tag{4.8b}$$

We call A_1 and A_2 areas in analogy to the two-level case where $A_1=\int_0^\tau\Omega_1(\tau',z)d\tau'$. Thus any explicit reference to the atomic variables is eliminated in this approximation

and we are left with two coupled nonlinear partial differential equations which refer only to the electric field envelopes of the laser pulses.

Each of these equations is similar in structure to the two-level result (the sine-Gordon equation[24]). In fact, setting $A_2=0$ in Eq. (4.8a) yields the usual equation. The cosine term is a modification of the polarization for the first pulse due to the fact that there is population transferred between levels 2 and 3. The sine-squared term in Eq. (4.8b) has a similar interpretation for the second pulse.

These equations are highly nonlinear and we cannot solve them in general analytically. We therefore must resort to computer calculations in most cases and results of the numerical integration of the equations are given in Sec. V. Nevertheless, it is clear that the equations are simpler to deal with and have fewer variables than the full Maxwell-Bloch equations. In addition to this, certain cases can be treated analytically, as shown in Sec. VI, and this general technique also allows the derivation of approximate area theorems in the inhomogeneously broadened case.

V. NUMERICAL INTEGRATION OF THE PARTIAL AREA EQUATIONS

It is evident from Eqs. (4.8) that a complicated relationship exists between the areas A_1 and A_2. Many three-level problems have been treated by two-level models in the past, and this interaction between the pulses has usually been ignored. It is possible that solutions to Eqs. (4.8) will show a significant modification of the corresponding two-level results. With this in mind, we will present our calculations in the following way. First the integration of the partial area equations will be compared to the numerical solution obtained by integrating the exact coupled Maxwell-Bloch equations [Eqs. (3.4) and (4.1)]. Next, where appropriate, comparisons will be given between the partial area equations and the corresponding two-level model. The two-level model used for comparisons will be that given by Burnham and Chiao[2] in which the second level is populated by a δ-function pulse excitation.

Figure 3 shows the comparison between the solutions of the partial area equations and of the Maxwell-Bloch equations for the cascade-A, cascade-B, Λ, and V configura-

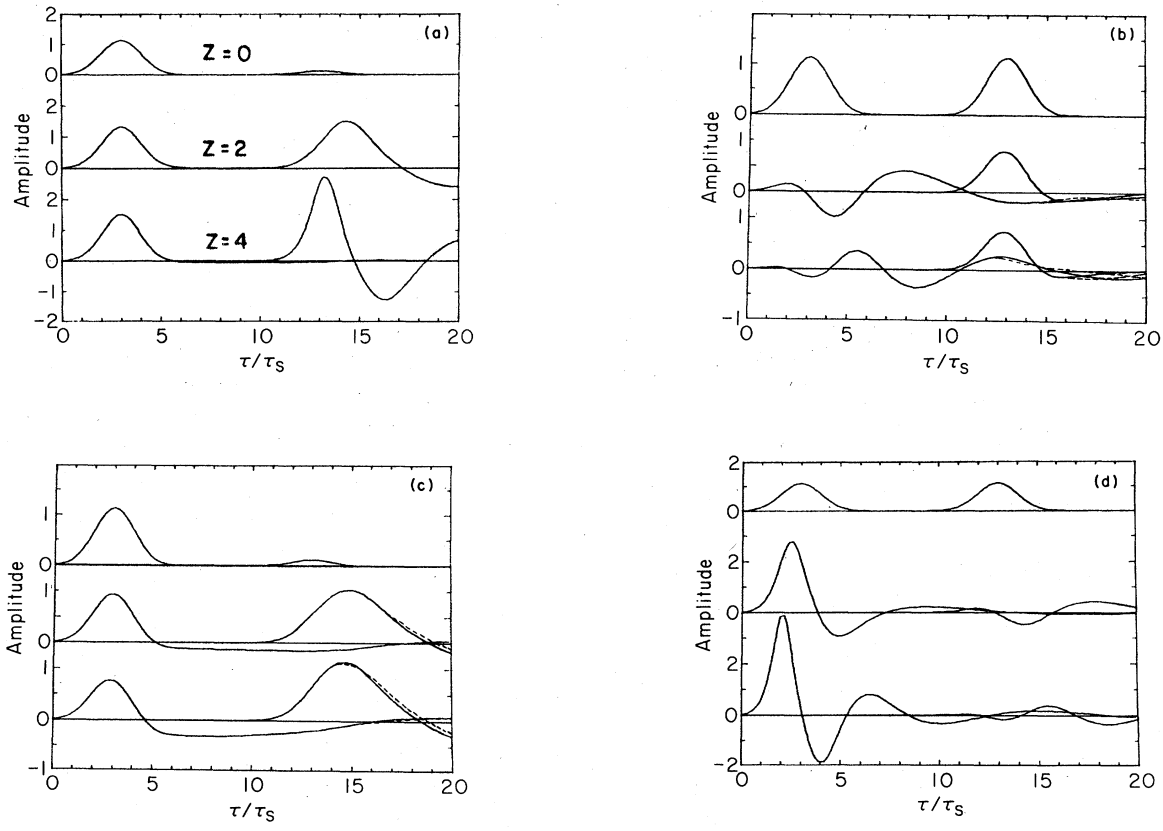

FIG. 3. Comparisons of the time evolution of the propagating pulses Ω_j predicted by the partial area equations [Eqs. (4.8)] to those given by the Maxwell-Bloch equations [Eqs. (3.4) and (4.1)] for the different level configurations for $Z=z\kappa_2\tau_s=0,2,4$. Input pulse envelopes are Gaussians with equal standard deviations τ_s: $\Omega_j(\tau)=\bar{\Omega}_j\exp\{-\frac{1}{2}[(\tau-\tau_j)/\tau_s]^2\}$ where $\bar{\Omega}_j$ is the peak amplitude of the jth pulse. Relative time delay of successive inputs is $10\tau_s$. Time is measured in units of τ_s. First pulse always has an initial area of 0.9π. Solid line is the Maxwell-Bloch result while the dashed line is the partial area result. Propagation distances for all plots are labeled as in (a). For each plot we list the configuration, initial area of the second pulse $[A_2(0)]$ and the gain ratio (κ_2/κ_1): (a) cascade A, $A_2(0)=0.1\pi$, $\kappa_2/\kappa_1=10$; (b) cascade B, $A_2(0)=0.9\pi$, $\kappa_2/\kappa_1=1$; (c) Λ, $A_2(0)=0.1\pi$, $\kappa_2/\kappa_1=10$; (d) V, $A_2(0)=0.9\pi$, $\kappa_2/\kappa_1=1$.

tions. The solid lines are the solutions of the exact equations while the dashed lines are the solutions of the approximate equations. We have chosen the initial area of the first pulse to give a large population transfer to the second level [$A_1(0)=0.9\pi$] so that the interaction between the pulses will be strong. The agreement between the two calculations is excellent. In fact, the dashed- and solid-line results for the V and cascade-A cases are virtually indistinguishable, which justifies in this and similar cases the use of the partial area equations.

The comparison to the Burnham-Chiao theory is given in Fig. 4, in the cascade-A and Λ cases. The Burnham-Chiao result is given by the dashed-dotted line. For the cascade-A case, all three theories give virtually identical results; however, for the Λ case the Burnham-Chiao result quickly deviates from the exact solution as the pulses propagate in z. The reason is easy to understand. Since the Burnham-Chiao theory acts as if the gain for the second transition were constant, it cannot take account of the dynamics of the first pulse which changes the gain. That the agreement is so good for the cascade-A case is also easy to explain. If we refer to Fig. 3(a) we see that the first pulse has hardly changed its shape during the propagation. The gain for the second pulse is thus, for all practical purposes, constant. Therefore all three theories give the same result. With longer propagation distances, however, the first pulse will eventually change significantly due to the amplification process. Then the Burnham-Chiao result will start to become noticeably different from

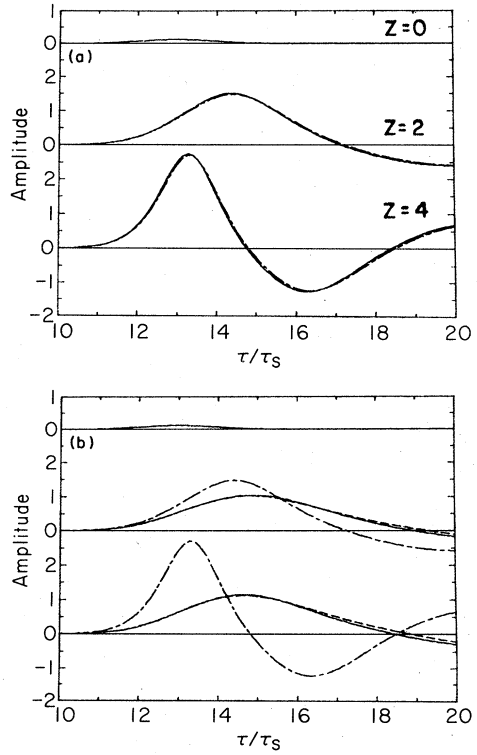

FIG. 4. Comparisons of the Maxwell-Bloch equations, the partial area equations, and the Burnham-Chiao two-level theory for the time development of the second pulse Ω_2. Parameters are the same as those given in Fig. 3. Dashed-dotted line is the Burnham-Chiao result. We have (a) cascade A and (b) Λ.

the other two theories. For the choice of parameters given in Fig. 3(a) this occurs at about $Z=8$.

It is fairly easy to predict when the Burnham-Chiao theory will give reasonable results and when it will not. Obviously, if the first pulse is sufficiently narrow and retains its initial area during the region of interest of propagation, the gain for the second level will be fairly constant. Then the two-level theory will give good results. If the area changes significantly, however, then so will the gain, and the evolution of the second pulse can be quite different from the Burnham-Chiao prediction.

The evolution of the first pulse is determined by the sine-Gordon equation

$$\frac{\partial^2}{\partial z\partial\tau}A_1=-s_1\frac{\kappa_1}{2}\sin A_1 \tag{5.1}$$

before the pulses start to overlap. Since the method of solution of this equation is known,[25] this information can be used to determine the change of area over the distance of propagation and therefore to predict when the Burnham-Chiao theory will break down.[26]

Even when the first pulse area does not change, the Burnham-Chiao theory will give incorrect results when the first pulse width is comparable to the time delay between the pulses. This will generally occur due to spatial evolution in transitions with gain since the first input tends to broaden, while the delay of the amplified output will reduce during propagation.

VI. APPLICATIONS TO SUPERFLUORESCENCE

The general superfluorescence problem is one of spontaneous emission from a group of atoms with a population inversion. This is a transient process occurring over time scales much shorter than one-atom spontaneous emission, for atoms sufficiently close together. Since superfluorescence is intrinsically quantum mechanical, we can no longer accurately describe the system by the semiclassical equations used in the preceding sections. We must now take into account the vacuum fluctuations which initiate the process. We can treat these fluctuations by using either operator equations of motion or operator representation theory. The latter choice allows us to derive equations which are formally similar to those of the semiclassical treatment and thus we can use the approximations made in Secs. III and IV to investigate the superfluorescence problem. This simplification is made by taking a coherent representation for both the field and atomic variables.

We will treat an open system without mirrors and take the active medium to be a large number of three-level atoms in a pencil-shaped volume, excited by a pump traveling in the $+\hat{z}$ direction. Under these circumstances, it has recently been shown that the quantum initiation and propagation of the superfluorescent radiation in the pump direction is described by the following propagation equation:[27]

$$\frac{\partial}{\partial z}\Omega_j(\vec{r})=\frac{i\lambda_j s_j}{4\pi}\nabla_\perp^2\Omega_j(\vec{r})-s_j\frac{2V_J}{\tau_j l}\delta^{(3)}(\vec{r}-\vec{r}_J)\psi_j^{J*}(\tau)\psi_{j+1}^J(\tau)\ , \tag{6.1}$$

where the coupling to any counterpropagating field is neglected and $\vec{r}_J$ is the center of a spatial volume V_J having N_J atomic inhabitants. The wavelength is λ_j for the jth transition, and l is the length of the superfluorescent medium which defines the relevant superfluorescence time:

$$\frac{1}{\tau_j}=\tfrac{1}{2}\kappa_j l \ . \tag{6.2}$$

We note here that κ_j,τ_j can be related to the Einstein A coefficient T_j^{-1} for the jth dipole transition as

$$\frac{1}{\tau_j}=3\lambda_j^2 nl/8\pi T_j \ , \qquad \kappa_j=3\lambda_j^2 n/4\pi T_j \ . \tag{6.3}$$

Here, Ω_j is the parameter which describes the coherent state of the jth field while the quantum state of the N_J atoms is represented by the SU(3) coherent-state vector $|\psi^J\rangle$ whose coefficients are given by the ψ_j^J's. It should be noted that, unlike the semiclassical case, the field $\vec{\mathscr{E}}_2$ must now be parallel to the 2-3 dipole since this is its source, and also the ψ_j^J's must now in general be taken to be complex to allow for random initial polarizations caused by the vacuum fluctuations.

The new feature which is not present in our previous equations is that the initial values of the coherent-state vectors are distributed in a δ-correlated way. The distribution is described by[27,28]

$$\langle \psi_m^J(0)\psi_n^{K*}(0)\rangle=\begin{cases}\frac{1}{N}\delta_{JK}\delta_{mn}, & m,n>1\\ 1+0(1/N), & m,n=1 \ .\end{cases} \tag{6.4}$$

Therefore, up to $0(1/N)$, the atomic coherent-state parameters ψ_j^J obey equations identical to Schrödinger's equations (3.4) and thus, to the same order of approximation, the partial area equations should hold for evolution from the initial state as long as the overlap is not large between the input and superfluorescent output fields.

For simplicity, we restrict our calculations to plane-wave propagation only. Thus the volumes V_J will be taken to extend over the full area of the superfluorescent pencil and only the average Rabi frequency will be computed after integrating over the pencil area A:

$$\Omega_j(z)=\frac{1}{A}\int\int \Omega_j(\vec{r})dx\,dy \ . \tag{6.5}$$

This approximation neglects diffraction out of the volume as well as transverse pump inhomogeneities. It is, however, approximately correct when the Fresnel number of the superfluorescent field $[A/(l\lambda)]$ is nearly unity and the pump is nearly uniform.

Next, in order to obtain analytic results, we suppose that the coupling coefficient κ_j is much larger in the superfluorescent than in the pump transition. Accordingly, the pump depletion will be negligible in a first approximation. The influence of the incoherent pulse on superfluorescence is discussed in Ref. 29, where the problem of quantum initiation of superfluorescence in a three-level medium is treated under the assumption of total separation of the pump pulse and the superfluorescence pulse.

Provided N_J is large, the polar and azimuthal angles, ϕ_1,ϕ_2 now have an extremely small initial value. Also, in the Jth volume V_J,

$$\langle \psi_i(0)\psi_j^*(0)\rangle=\frac{\delta_{ij}}{N}, \quad i,j>1 \ . \tag{6.6}$$

However, the result of Eqs. (3.7) is obtainable from integrating Eqs. (3.5) just as before, except with a correction due to the initial value. Hence, for $|\psi_3|\ll 1$, we obtain

$$\psi_3(\tau)=\psi_3(0)+\int_0^\tau \frac{\Omega_2(\tau')}{2}\sin\phi_1(\tau')d\tau' \ , \tag{6.7}$$

where $\phi_1(\tau)$ is given by Eq. (3.7a).

Here, given a large pump area ϕ_1, the initial value $\psi_2(0)$ has a negligible effect and can be ignored. On the other hand, $\psi_3(0)$ greatly modifies the effective rotation due to $\Omega_2(\tau)$, which initially has a very small partial area. However, $\psi_3(0)$ is complex valued. This implies that Ω_2 must be taken as complex also. Provided only a linear approximation is employed for Ω_2, this does not change the resulting equations which are now

$$\psi_3^J(\tau)=\psi_3^J(0)+\int_0^\tau \frac{\Omega_2(\tau',z)}{2}\sin\left[\frac{A_1(\tau')}{2}\right]d\tau' \ , \tag{6.8a}$$

$$\tau_2\frac{\partial}{\partial z}\Omega_2(\tau,z)=2\left[\frac{\Delta l}{l}\right]\sum_J \delta(z-z_J)\psi_3^J(\tau)\sin\left[\frac{A_1(\tau)}{2}\right] \ . \tag{6.8b}$$

Here, Δl is the length of the volume element V_J and we have taken the second transition to be amplifying ($s_2=-1$). Next, taking the formal limit of $\Delta l\to 0$ and changing to new variables Z and T,

$$Z=z/l, \quad T=\frac{1}{\tau_2}\int_0^\tau \sin^2\left[\frac{A_1(\tau')}{2}\right]d\tau' \ , \tag{6.9}$$

we obtain the final equations

$$\frac{\partial^2}{\partial Z\partial T}A_2(T,Z)\simeq A_2(T,Z)+A_0(Z) \ , \tag{6.10a}$$

$$\langle A_0(Z)A_0^*(Z')\rangle=\frac{4}{N}\delta(Z-Z') \ , \tag{6.10b}$$

where

$$A_2(T,Z)=\int_0^T \tau_2\Omega_2(T')\csc\left[\frac{A_1(T')}{2}\right]dT' \ . \tag{6.10c}$$

We note, however, that the description of Eqs. (6.8) with the volume cells is physically preferable as it shows precisely how the physical space is divided. Equations (6.10) can be used directly since they, in fact, give exactly the same final equation. The crucial difference is in the redefinition of the time in terms of Ω_1. If the usual crossing-time criterion for superfluorescent delay time were replaced by a criterion for $A_2(T,Z)=A_c$ as defined in Eq. (6.10c), then it is clear that the effect of optical pumping is to lengthen the delay time via the rescaling integral in Eq. (6.9). In particular, if the equivalent two-

level delay time were τ_D and the pump turned on and off at $\tau=0$ and $\tau=\tau_P$, respectively, the three-level delay time would be implicitly defined by τ_{D3} where

$$\frac{\tau_2}{4}\ln(A_c\sqrt{2\pi N})^2=\tau_D=\int_0^{\tau_{D3}}\sin^2\left[\frac{A_1(\tau')}{2}\right]d\tau' \quad (6.11a)$$

or

$$\tau_{D3}=\csc^2\left[\frac{A_1(\tau_p)}{2}\right]\left[\tau_D-\int_0^{\tau_p}\sin^2\left[\frac{A_1(\tau')}{2}\right]d\tau'\right]+\tau_p\ ,$$
$$\tau_{D3}>\tau_p\ . \quad (6.11b)$$

Clearly, for an odd multiple of π input, short compared to τ_D, there is no effect since then $\sin^2[A_1(\tau_p)/2]\simeq 1$. On the other hand, for a short pump pulse whose area is equal to an even multiple of π, the delay is greatly lengthened. In the case of a temporally uniform pump of Rabi frequency Ω_p we have (with $A_1=\Omega_p\tau_p$)

$$\tau_D=\tfrac{1}{2}\left[\tau_{D3}-\frac{\sin(\Omega_p\tau_{D3})}{\Omega_p}\right],\quad \tau_{D3}<\tau_p \quad (6.12a)$$

or

$$\tau_{D3}=\csc^2\left[\frac{A_1}{2}\right]\left[\tau_D-\frac{\tau_p}{2}+\frac{\sin(A_1)}{2\Omega_p}\right]+\tau_p\ ,$$
$$\tau_{D3}>\tau_p\ . \quad (6.12b)$$

Thus, the overall effect in this case is a lengthening of the delay on the average together with a temporal modulation at the Rabi frequency of the pump. Note that the results above are restricted to the delay involved in the linear or initiation region of superfluorescence, not the final nonlinear peak. This implies that they strictly hold for $A_c\ll 1$. However, as a first step, we can use $A_c=1$ to obtain τ_D in Eqs. (6.11) and (6.12), giving the approximate delay at the peak of the superfluorescent output which was not given in previous analyses. Finally, the transformation outlined here generally is useful in giving equations of the usual two-level type as a description of a three-level system. This is a different transformation to that already employed for Raman-type experiments[30,31] and can obviously permit the direct calculation of the output intensity, correlations, and pulse statistics, as well as the delay time, to extend previous results on the three-level problem.[32] We note, since we have made the assumption of a plane-wave pump, that to analyze practical experiments, we would need to perform numerical calculations.

VII. AREA THEOREMS

When we include Doppler broadening in the system, we must allow for the fact that all the atoms will no longer be tuned on resonance due to their different velocity components. We must then generalize the interaction Hamiltonian to include detunings. We therefore get

$$\hat{V}_I(t,\Delta,\Delta')=\frac{i\hbar}{2}[(\Omega_1 e^{-i\Delta t}\hat{\sigma}_{21}+\Omega_2 e^{-i\Delta' t}\hat{\sigma}_{32})-\text{H.c.}]\ , \quad (7.1)$$

where

$$\Delta=s_1|\omega|-\omega_{21},\quad \Delta'=s_2|\omega'|-\omega_{32}\ . \quad (7.2)$$

The analysis of Secs. II and III does not carry through for this case since now $\hat{V}_I$ cannot be written solely in terms of the angular momentum operators $\hat{I}_1$, $\hat{I}_2$, and $\hat{I}_3$. We will attempt, therefore, to simplify the analysis of the system by deriving area theorems analogous to that of McCall and Hahn[33] by integrating the Maxwell equations in time.

The Maxwell equations become

$$\frac{\partial}{\partial\xi}\Omega_1+\frac{1}{c}\frac{\partial}{\partial t}\Omega_1=-s_1\kappa_1\langle\sigma_{12}e^{-i\Delta t}\rangle_\Delta\ , \quad (7.3a)$$

$$\frac{\partial}{\partial\xi}\Omega_2+\frac{1}{c}\frac{\partial}{\partial t}\Omega_2=-s_2\kappa_2\langle\sigma_{23}e^{-i\Delta' t}\rangle_{\Delta'}\ , \quad (7.3b)$$

where $\langle\ \rangle_{\Delta,\Delta'}$ denotes the averaging over the detunings (instead of the velocities), and we write $\langle\hat{\sigma}_{12}\rangle=\sigma_{12}$, etc., for the quantum expectation. We still concern ourselves only with times during which we can ignore effects of homogeneous broadening and natural relaxation processes. We will perform our calculations for Ω_1. The analysis proceeds similarly for Ω_2.

Integrating Eq. (7.3a) in time gives

$$\int_0^t\left[\frac{\partial}{\partial\xi}\Omega_1+\frac{1}{c}\frac{\partial}{\partial t'}\Omega_1\right]dt'=-s_1\kappa_1\int_0^t\langle\sigma_{12}e^{i\Delta t'}\rangle_\Delta dt'\ . \quad (7.4)$$

If we choose $t\geq\xi$ where ξ is a time such that $\Omega_1(t\geq\xi)=\Omega_2(t\geq\xi)=0$, we may split up Eq. (7.4) into two parts:

$$\int_0^\xi\left[\frac{\partial}{\partial\xi}\Omega_1+\frac{1}{c}\frac{\partial}{\partial t'}\Omega_1\right]dt'=-s_1\kappa_1\int_0^\xi\langle\sigma_{12}e^{i\Delta t'}\rangle_\Delta dt'\ , \quad (7.5a)$$

$$\int_\xi^t\left[\frac{\partial}{\partial\xi}\Omega_1+\frac{1}{c}\frac{\partial}{\partial t'}\Omega_1\right]dt'=-s_1\kappa_1\int_\xi^t\langle\sigma_{12}e^{i\Delta t'}\rangle_\Delta dt'\ . \quad (7.5b)$$

The left-hand side (lhs) of Eq. (7.5b) is zero since $\Omega_1(t'\geq\xi)=0$. Also, $\sigma_{12}(t'\geq\xi,\Delta)=\sigma_{12}(\xi,\Delta)$ since $|\psi(t'\geq\xi)\rangle=|\psi(\xi)\rangle$ from the Schrödinger equation. Thus we get

$$\int_\xi^t\langle\sigma_{12}(\xi,\Delta)e^{i\Delta t'}\rangle_\Delta dt'=0\ . \quad (7.6)$$

The integration gives

$$\left\langle\sigma_{12}(\xi,\Delta)e^{i\Delta\xi}\frac{(e^{i\Delta(t-\xi)}-1)}{\Delta}\right\rangle_\Delta=0\ . \quad (7.7)$$

Since this is true for any $t\geq\xi$, we can let $t\to\infty$ and then using the well-known limit[34]

$$\lim_{t\to\infty}\frac{(1-e^{i\Delta(t-\xi)})}{\Delta}=\mathrm{P}\left[\frac{1}{\Delta}\right]-i\pi\delta(\Delta) \quad (7.8)$$

we find

$$-i\mathrm{P}\left\langle\frac{\sigma_{12}(\xi,\Delta)e^{i\Delta\xi}}{\Delta}\right\rangle_\Delta=\langle\sigma_{12}(\xi,\Delta)e^{i\Delta\xi}\pi\delta(\Delta)\rangle_\Delta$$
$$=\pi g_{21}(0)\sigma_{12}(\xi,\Delta=0)\ , \qquad (7.9)$$

where $g_{21}(\Delta)$ is the weighting function for the detuning for the $1\leftrightarrow2$ transition.

The lhs of Eq. (7.5a) integrates to $\int_0^\xi(\partial/\partial\xi)\Omega_1 dt'$ since we take $\Omega_1(t\leq0)=0$. Upon integrating the right-hand side (rhs) by parts we find

$$\int_0^\xi\langle\sigma_{12}e^{i\Delta t'}\rangle_\Delta dt'=-i\left\langle\sigma_{12}(\xi,\Delta)\frac{e^{i\Delta\xi}}{\Delta}\right\rangle_\Delta+i\int_0^\xi\left\langle\left[\frac{\partial}{\partial t'}\sigma_{12}\right]\frac{e^{i\Delta t'}}{\Delta}\right\rangle_\Delta dt'$$
$$=\pi g_{21}(0)\sigma_{12}(\xi,\Delta=0)+i\int_0^\xi\left\langle\left[\frac{\partial}{\partial t'}\sigma_{12}\right]\frac{e^{i\Delta t'}}{\Delta}\right\rangle_\Delta dt'\ . \qquad (7.10)$$

We may compute $(\partial/\partial t')\sigma_{12}(t',\Delta)$ from

$$\frac{\partial}{\partial t'}\sigma_{12}(t',\Delta)=\frac{1}{i\hbar}\langle[\hat\sigma_{12},\hat V_I]\rangle$$
$$=\tfrac{1}{2}[\Omega_1e^{-i\Delta t'}(\sigma_{11}-\sigma_{22})-\Omega_2^*e^{i\Delta' t'}\sigma_{13}]\ . \qquad (7.11)$$

Thus the integral on the rhs of Eq. (7.10) becomes

$$i\int_0^\xi\left\langle\left[\frac{\partial}{\partial t'}\sigma_{12}(t',\Delta)\right]\frac{e^{i\Delta t'}}{\Delta}\right\rangle_\Delta dt'$$
$$=\frac{i}{2}\int_0^\xi\langle\Omega_1(\sigma_{11}-\sigma_{22})/\Delta\rangle_\Delta dt'$$
$$-\frac{i}{2}\int_0^\xi\left\langle\Omega_2^*\sigma_{13}\frac{e^{i(\Delta+\Delta')t'}}{\Delta}\right\rangle_\Delta dt'\ . \qquad (7.12)$$

It is shown in Appendix A that if initially Ω_1 and Ω_2 are real, they remain real throughout the propagation. Thus

$$\frac{i}{2}\int_0^\xi\langle\Omega_1(\sigma_{11}-\sigma_{22})/\Delta\rangle_\Delta dt'$$

must give no contribution since it is entirely imaginary (it is, in fact, zero). Therefore

$$\int_0^\xi\langle\sigma_{12}e^{i\Delta t'}\rangle_\Delta dt'$$
$$=\pi g_{21}(0)\sigma_{12}(\xi,\Delta=0)$$
$$-\frac{i}{2}\int_0^\xi\left\langle\Omega_2\sigma_{13}\frac{e^{i(\Delta+\Delta')t'}}{\Delta}\right\rangle_\Delta dt'\ . \qquad (7.13)$$

We cannot evaluate the integral on the rhs in Eq. (7.13) but we may approximate it for two special cases.

Case I. The separation between the pulses is much longer than T_{21}^*, the inhomogeneous lifetime for the $1\leftrightarrow2$ transition. In this case the contribution of the integral will be negligible. This can be seen from the fact that in this regime the source for Ω_1, namely $\langle\sigma_{12}e^{i\Delta t}\rangle_\Delta$, will have decayed to near zero by the time Ω_2 arrives so that the second pulse causes a negligible modification of the time development of the σ_{12} dipole.

Case II. The pulse widths and separation are much shorter than T_{21}^* and the first and third levels are degenerate (or nearly so). In this case the integral will also be negligible. The reason for this is that the detuning distribution will be very sharply peaked around $\Delta=0$ so that we may approximate

$$\left\langle\sigma_{13}(t,\Delta)\frac{e^{i(\Delta+\Delta')t}}{\Delta}\right\rangle_\Delta$$
$$\simeq\sigma_{13}(t,0)\left\langle\frac{e^{i(\Delta+\Delta')t}}{\Delta}\right\rangle_\Delta$$
$$=\sigma_{13}(t,0)iT_{21}^*\mathrm{erf}\left[\frac{t}{T_{21}^*}\frac{\omega_{31}}{2\sqrt{\pi}\omega_{21}}\right]=0 \qquad (7.14)$$

since $\omega_{31}=0$ when the levels are degenerate. Here we have used the definition $T_{21}^*=\pi g_{21}(0)$ and the relation $\Delta'/\Delta=\omega_{32}/\omega_{21}$.

Thus for both cases we may write

$$\int_0^\xi\langle\sigma_{12}e^{i\Delta t'}\rangle_\Delta dt'\simeq T_{21}^*\sigma_{12}(\xi,\Delta=0)\ . \qquad (7.15)$$

In full we thus have

$$\int_0^\Xi\frac{\partial}{\partial z}\Omega_1 d\tau'\simeq-s_1\kappa_1T_{21}^*\sigma_{12}(\Xi,\Delta=0)$$
$$=-s_1\alpha_1\sigma_{12}(\Xi,\Delta=0) \qquad (7.16)$$

for cases I and II. $\alpha_1=\pi\mathcal{N}|\vec d_{21}\cdot\vec\epsilon_1|^2|\omega|g_{21}(0)/\epsilon_0\hbar c$ is the Beer's absorption coefficient for the $1\leftrightarrow2$ transition. Here we have transformed to the moving frame and let $\xi\rightarrow\Xi$.

Similar calculations for Ω_2 yield

$$\int_0^\Xi\frac{\partial}{\partial z}\Omega_2 d\tau'\simeq-s_2\kappa_2T_{32}^*\sigma_{23}(\Xi,\Delta'=0)$$
$$=-s_2\alpha_2\sigma_{23}(\Xi,\Delta'=0) \qquad (7.17)$$

for both cases. Here $T_{32}^*=\pi g_{32}(0)$ is the inhomogeneous lifetime for the $2\leftrightarrow3$ transition and α_2 is the Beer's absorption coefficient for the second pulse.

In the case where the pulses obey the small-overlap approximation, we may use the results of Sec. IV. In terms of the angles ϕ_1 and ϕ_2 we then have the following.

Case I. Equation (4.4a) reduces to

$$\sigma_{12}(\Xi,\Delta=0)=\tfrac{1}{2}\sin[2\phi_1(\Xi)] \qquad (7.18a)$$

since the second pulse will not modify this polarization, while Eq. (4.4b) remains unchanged:

$$\sigma_{23}(\Xi, \Delta'=0)=\tfrac{1}{2}\sin^2\phi_1(\Xi)\sin[2\phi_2(\Xi)] . \tag{7.18b}$$

Case II. Here Eqs. (4.4) will remain unchanged. Therefore

$$\sigma_{12}(\Xi, \Delta=0)=\tfrac{1}{2}\sin[2\phi_1(\Xi)]\cos\phi_2(\Xi) , \tag{7.19a}$$

$$\sigma_{23}(\Xi, \Delta'=0)=\tfrac{1}{2}\sin^2\phi_1(\Xi)\sin[2\phi_2(\Xi)] . \tag{7.19b}$$

If we now rewrite the pulses Ω_1 and Ω_2 in terms of the areas defined by Eq. (4.7) through the relations given in Eqs. (4.5), we may obtain the following equations for the areas.

Case I. We have

$$\frac{\partial}{\partial z}A_1\simeq -s_1\frac{\alpha_1}{2}\sin A_1 , \tag{7.20a}$$

$$\frac{\partial}{\partial z}A_2\simeq -s_2\frac{\alpha_2}{2}\sin^2\left[\frac{A_1}{2}\right]\sin A_2 . \tag{7.20b}$$

Case II. We have

$$\frac{\partial}{\partial z}A_1\simeq -s_1\frac{\alpha_1}{2}\sin A_1\cos\left[\frac{A_2}{2}\right] , \tag{7.21a}$$

$$\begin{aligned}\frac{\partial}{\partial z}\left[A_2\sin\left[\frac{A_1}{2}\right]\right] &\simeq \sin\left[\frac{A_1}{2}\right]\left[-s_2\frac{\alpha_2}{2}\sin^2\left[\frac{A_1}{2}\right]\sin A_2\right. \\ &\left. -s_1\alpha_1\cos^2\left[\frac{A_1}{2}\right]\sin\left[\frac{A_2}{2}\right]\right] .\end{aligned} \tag{7.21b}$$

These calculations are carried out in Appendix B.

Equations (7.20) have a simple interpretation. Since the second pulse does not modify the polarization of the first pulse, Eq. (7.20a) is just the familiar two-level area theorem of McCall and Hahn. Equation (7.20b) is also a two-level area theorem but with a z-dependent absorption coefficient: $-s_2(\alpha_1/2)\sin^2(A_1/2)$. This is merely a reflection of the fact that not all the population is available for interaction with the second pulse. The $\sin^2(A_1/2)$ term is a measure of how much population has been transferred to the second level by the first pulse before the second pulse arrives.

We may integrate Eqs. (7.20) by elementary means to obtain the solutions

$$\tan\left[\frac{A_1(z)}{2}\right]=\tan\left[\frac{A_1(0)}{2}\right]\exp\left[-s_1\frac{\alpha_1}{2}z\right], \tag{7.22a}$$

$$\begin{aligned}\tan\left[\frac{A_2(z)}{2}\right] &=\tan\left[\frac{A_2(0)}{2}\right] \\ &\times\left[\cos^2\left[\frac{A_1(0)}{2}\right]+\sin^2\left[\frac{A_1(0)}{2}\right]e^{-s_1\alpha_1 z}\right]^{s_1s_2(\alpha_2/2\alpha_1)}\end{aligned} \tag{7.22b}$$

We will concentrate our discussion on the second equation since the first is well known.[33].

Two special cases present themselves at once. The first is when $A_1(0)$ is an integral multiple of 2π.[35] Equation (7.22b) then states that the area of the second pulse remains unchanged during the propagation. This is just a consequence of the well known result that a $2n\pi$ area pulse will return the population to its initial state so that the second pulse will have nothing to interact with.

When the first pulse has an initial area $A_1(0)=\pm(2n+1)\pi$, Eq. (7.22b) reduces to

$$\tan\left[\frac{A_2(z)}{2}\right]=\tan\left[\frac{A_2(0)}{2}\right]\exp\left[-s_2\frac{\alpha_2}{2}z\right] \tag{7.23}$$

which is just the solution to a two-level problem. That this is so is evident from the fact that a $(2n+1)\pi$ area pulse will completely transfer the population from the first to the second level.

To discuss the asymptotic limit $z\to\infty$ we must classify the system according to which transitions are absorbing ($s_i=+1$) and which are amplifying ($s_i=-1$). The limits are easily computed and we give them in Table I.

The interpretation of these limits is most easily made if we perform an analysis in the A_1-A_2 phase plane. Since the system is autonomous, we may eliminate the z variable by dividing Eq. (7.20b) by Eq. (7.20a) to obtain

$$\frac{dA_2}{dA_1}=s_1s_2\frac{\alpha_1}{2\alpha_2}\tan\left[\frac{A_1}{2}\right]\sin(A_2) . \tag{7.24}$$

We see that the form of the solution will depend only on the product of signs s_1s_2. However, we will find that the physical development of the system will depend strongly on which transitions are amplifying and which absorbing.

TABLE I. Asymptotic limits of $\tan[A_2(z)/2]$ for the first set of area equations [Eqs. (7.20)]. These are obtained by taking the limit $z\to\infty$ in Eq. (7.22b).

	$s_2=+1$	$s_2=-1$
$s_1=+1$	$\tan\left[\frac{A_2(0)}{2}\right]\left[\cos\left[\frac{A_1(0)}{2}\right]\right]^{\alpha_2/2\alpha_1}$	$\tan\left[\frac{A_2(0)}{2}\right]\left[\sec\left[\frac{A_1(0)}{2}\right]\right]^{\alpha_2/2\alpha_1}$
$s_1=-1$	0	∞

TABLE II. Asymptotic limits of $A_2(z)$ for the first set of area equations [Eqs. (7.20)]. These limits are obtained from Eq. (7.22b) with the help of the phase plot Fig. 5 to set the proper period. Tan^{-1} denotes the principal value of the arctangent.

	$s_2=+1$	$s_2=-1$
$s_1=+1$	$(2n-1)\pi<A_2(0)<(2n+1)\pi$ $2\,\mathrm{Tan}^{-1}\left\{\tan\left[\frac{A_2(0)}{2}\right]\times\left[\cos\left[\frac{A_1(0)}{2}\right]\right]^{\alpha_2/2\alpha_1}\right\}+2n\pi$	$(2n-1)\pi<A_2(0)<(2n+1)\pi$ $2\,\mathrm{Tan}^{-1}\left\{\tan\left[\frac{A_2(0)}{2}\right]\times\left[\sec\left[\frac{A_1(0)}{2}\right]\right]^{\alpha_2/2\alpha_1}\right\}+2n\pi$
$s_1=-1$	$(2n-1)\pi<A_2(0)<(2n+1)\pi$ $2n\pi$	$2n\pi<A_2(0)<(2n+2)\pi$ $(2n+1)\pi$

Solutions of Eq. (7.24) are plotted in Fig. 5 for different configurations. We show (a) $s_1=-1$, $s_2=-1$ (cascade A), and (b) $s_1=-1$, $s_2=+1$ (V). The graphs for the cascade-B and Λ cases are identical to those for cascade A and V, respectively, except that the direction arrows are reversed. The plots are done with a gain ratio of $\alpha_2/\alpha_1=2$.

It is well known in the two-level theory (applicable to the first pulse) that when the transition is absorbing, $(2n+1)\pi$ area pulses are unstable and pulses with initial areas near odd multiples of π will tend toward areas of even multiples of π. For an amplifying transition just the opposite is true. $2n\pi$ area pulses are unstable and pulses with initial areas near $2n\pi$ will tend toward $(2n+1)\pi$ or $(2n-1)\pi$ areas. This information allows us to draw the direction arrows on the plots to show the development of the area of the second pulse for the different configurations. We can see from the phase plots that, for the cascade-B and Λ cases, we can have the second pulse approach any desired area if we choose the initial conditions appropriately.

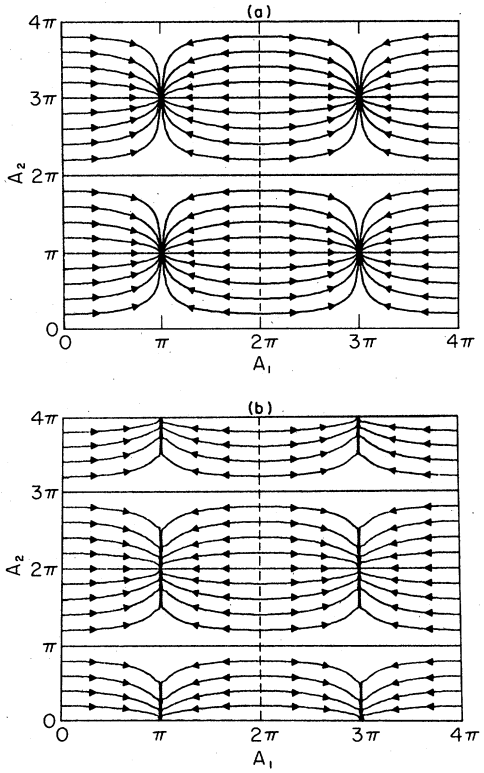

FIG. 5. Phase plot of A_2 vs A_1 for the first set of area equations [Eqs. (7.20)]. Gain ratio is $\alpha_2/\alpha_1=2$. Arrows show the direction of the development of the different systems. We have (a) cascade A, (b) V. The patterns are repeated periodically throughout the entire A_1-A_2 plane with period 2π in both directions. Plots for the cascade-B and Λ cases are identical to (a) and (b), respectively, with the direction arrows reversed.

Table II is an extension of Table I and summarizes the asymptotic limits of $A_2(z)$. We give a comparison of the area theorem Eqs. (7.20) to the numerically integrated Maxwell-Bloch equations for the Λ case in Fig. 6.

Equations (7.21) are not as amenable to analysis as Eqs. (7.20). We are unable to solve them analytically; however, we may still perform an analysis in the phase plane. Equations (7.21) form an autonomous system so that dividing Eq. (7.21b) by Eq. (7.21a) we may derive

$$\frac{dA_2}{dA_1}=s_2s_1\frac{\alpha_2}{\alpha_1}\tan\left[\frac{A_1}{2}\right]\sin\left[\frac{A_2}{2}\right]+\cot\left[\frac{A_1}{2}\right]\left[\tan\left[\frac{A_2}{2}\right]-\left[\frac{A_2}{2}\right]\right]. \quad (7.25)$$

Solutions of Eq. (7.25) are given in Fig. 7 for the Λ con-

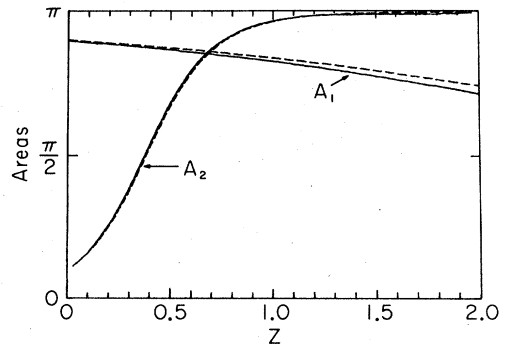

FIG. 6. Comparison of the area theorem Eqs. (7.22) to the integrated Maxwell-Bloch equations for the Λ case. The parameters are the same as those given in Fig. 3(c). In addition we have $T_{21}^*=2\tau_s$. The areas are plotted for distances $Z=z\kappa_1 T_{21}^*=0$ through $Z=2$.

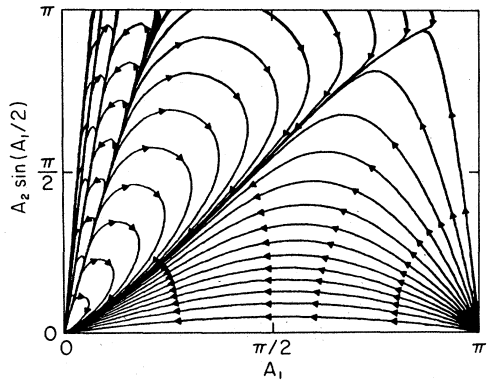

FIG. 7. Phase plot of $A_2\sin(A_1/2)$ vs A_1 for the second set of area equations [Eqs. (7.21)] for the Λ configuration. Gain ratio is $\alpha_2/\alpha_1=1$. Direction of development of the system is shown by the arrows. Plot is the same for the V configuration except that the arrows are reversed.

figuration. For the V case, the direction arrows are reversed. The gain ratio is $\alpha_2/\alpha_1=1$. The cascade cases are not shown since for those configurations we cannot have the $|1\rangle$ and $|3\rangle$ levels degenerate. The value

$$A_2\sin(A_1/2)=\int_0^{\Xi}\Omega_2(\tau')\sin[A_1(\tau')/2]d\tau'$$

is plotted since this corresponds most closely with the area of the second pulse for this case. We give a comparison to the numerically integrated Maxwell-Bloch equations in Fig. 8 for the V case.

We have found from computer runs that in the regions of the phase diagram where the integral curves resemble folia, the predictions of this area theorem can be poor. This is due largely to the fact that in these regions, $A_2(0)$ will generally be large [$A_2(0)\gtrsim\pi$] and the small-overlap assumption will break down. This is especially true for the V case where the first pulse increases its area during propagation by developing a large positive tail.

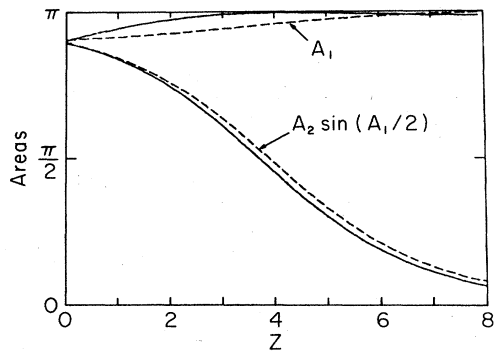

FIG. 8. Comparison of the predictions of the area equations Eqs. (7.21) to the integrated Maxwell-Bloch equations for the V case. Parameters are the same as those given in Fig. 3(d) except that the relative time delay between pulses is $5\tau_s$. In addition we have $T_{21}^*=10\tau_s$. Areas are plotted for distances $Z=z\kappa_1 T_{21}^*=0$ through $Z=8$.

VIII. SUMMARY

We have investigated, both analytically and numerically, coherent propagation in a three-level system when the pump and probe pulses have a small overlap. We have taken advantage of the fact that the on-resonance Hamiltonian can be written in terms of angular momentum operators by defining two rotation angles to describe the time evolution of the atomic system. The small-overlap assumption was used to rewrite Maxwell's equations in terms of these angles.

Numerical computations show that the partial area equations obtained describe the system very well as long as the small-overlap assumption is satisfied. The calculation for superfluorescence predicts a lengthening of the superfluorescent delay time for the cases where the pump pulse does not completely invert the system.

Although the Hamiltonian for the off-resonance case cannot be written solely in terms of angular momentum operators, we have taken advantage of the Doppler averaging to find approximate equations for the time integrated pulse areas for two special cases: (a) a very broad line, and (b) a very narrow line where the first and third levels are degenerate. The broad-line case is equivalent to two successive applications of the McCall-Hahn area theorem—the first pulse sets up the initial conditions for the second pulse by transferring population into the second level. We know of no analogy in the literature for the narrow-line case.

ACKNOWLEDGMENTS

The research reported here was partially supported by the U.S. Department of Energy. P.D.D. acknowledges support from the Allied Corporation.

APPENDIX A

In this appendix we show that, for the Doppler-broadened system, if the Rabi frequencies Ω_1 and Ω_2 are initially real they will remain real throughout the propagation. From Eqs. (7.3) this means that we must show that the driving dipoles of the fields remain real. In order to do this we first look at the equations of motion for the state vector $|\psi(t,\Delta,\Delta')\rangle$:

$$i\hbar\frac{\partial}{\partial t}|\psi(t,\Delta,\Delta')\rangle=\hat{V}_I(t,\Delta,\Delta')|\psi(t,\Delta,\Delta')\rangle\ , \qquad \text{(A1)}$$

where $\hat{V}_I(t,\Delta,\Delta')$ is given by Eq. (7.1). If we assume that the Rabi frequencies are real, then this gives directly

$$\frac{\partial}{\partial t}|\psi(t,\Delta,\Delta')\rangle = \tfrac{1}{2}[\Omega_1(e^{-i\Delta t}\hat{\sigma}_{21}-e^{i\Delta t}\hat{\sigma}_{12}) + \Omega_2(e^{-i\Delta' t}\hat{\sigma}_{32}-e^{i\Delta' t}\hat{\sigma}_{23})]|\psi(t,\Delta,\Delta')\rangle\ . \qquad \text{(A2)}$$

The equation of motion for the expectation value of an atomic operator is then given by

$$\frac{\partial}{\partial t}\langle\hat{\sigma}_{jk}\rangle=\frac{1}{i\hbar}\langle\psi(t,\Delta,\Delta')|[\hat{\sigma}_{jk},\hat{V}_I]|\psi(t,\Delta,\Delta')\rangle\ . \qquad \text{(A3)}$$

Performing this calculation gives

$$\frac{\partial}{\partial t}\langle\hat{\sigma}_{jk}\rangle=\tfrac{1}{2}\{\Omega_1[e^{-i\Delta t}(\langle\hat{\sigma}_{j1}\rangle\delta_{k2}-\langle\hat{\sigma}_{k2}\rangle\delta_{j1})-e^{i\Delta t}(\langle\hat{\sigma}_{j2}\rangle\delta_{k1}-\langle\hat{\sigma}_{k1}\rangle\delta_{j2})]$$
$$+\Omega_2[e^{-i\Delta' t}(\langle\hat{\sigma}_{j2}\rangle\delta_{k3}-\langle\hat{\sigma}_{k3}\rangle\delta_{j2})-e^{i\Delta' t}(\langle\hat{\sigma}_{j3}\rangle\delta_{k2}-\langle\hat{\sigma}_{k2}\rangle\delta_{j3})]\}\ . \tag{A4}$$

Now if we set $\Delta\rightarrow-\Delta$ (and simultaneously $\Delta'\rightarrow-\Delta'$ since Δ' is proportional to Δ) then this equation remains invariant if we require $\sigma_{jk}(t,\Delta,\Delta')=\sigma^*_{jk}(t,-\Delta,-\Delta')$ for real Rabi frequencies. Now the driving term for the first field is given by $\langle\sigma_{12}(t,\Delta)e^{i\Delta t}\rangle_\Delta$. Using the above symmetry relation, we obtain for the imaginary part of the dipole

$$\mathrm{Im}\langle\sigma_{12}(t,\Delta)e^{i\Delta t}\rangle_\Delta=\mathrm{Im}\int_{-\infty}^{\infty}d\Delta\, g_{21}(\Delta)\sigma_{12}(t,\Delta)e^{i\Delta t}=\mathrm{Im}\int_0^{\infty}d\Delta\, g_{21}(\Delta)[\sigma_{12}(t,\Delta)e^{i\Delta t}+\sigma_{12}(t,-\Delta)e^{-i\Delta t}]$$
$$=\mathrm{Im}\int_0^{\infty}d\Delta\, g_{21}(\Delta)[\sigma_{12}(t,\Delta)e^{i\Delta t}+\text{c.c.}]=0 \tag{A5}$$

since the rhs is entirely real. We have used the fact that the detuning function $g(\Delta)$ is symmetric about $\Delta=0$. A similar calculation shows

$$\mathrm{Im}\langle\sigma_{23}(t,\Delta')e^{i\Delta' t}\rangle_{\Delta'}=0\ . \tag{A6}$$

Thus if the Rabi frequencies start out real, the driving terms never develop imaginary parts and so the field envelopes remain real throughout the propagation.

APPENDIX B

Here we perform the calculations which explicitly give the area equations in Eqs. (7.20) and (7.21) for small overlap of the pulses. Combining Eqs. (3.7a) and (7.16) yields immediately

$$\frac{\partial}{\partial z}\phi_1=-s_1\frac{\alpha_1}{2}\sigma_{12}(\Xi,\Delta=0)\ . \tag{B1}$$

For the second pulse, we look at Eq. (3.7b). For case I, $\sin\phi_1(\tau)$ will have reached a steady value by the time the second pulse comes along and thus we may pull this factor out of the integral to obtain

$$\phi_2(\Xi)=\int_0^{\Xi}\frac{\Omega_2(\tau')}{2}d\tau'\ . \tag{B2}$$

Combining this with Eq. (7.17) yields

$$\frac{\partial}{\partial z}\phi_2\simeq-s_2\frac{\alpha_2}{2}\sigma_{23}(\Xi,\Delta'=0)\ . \tag{B3}$$

For the second case we proceed by differentiating $\phi_2\sin\phi_1$ and using Eq. (3.7b):

$$\left[\frac{\partial}{\partial\xi}+\frac{1}{c}\frac{\partial}{\partial t}\right]\phi_2\sin\phi_1$$
$$=\left[\frac{\partial}{\partial\xi}+\frac{1}{c}\frac{\partial}{\partial t}\right]\int_0^t\frac{\Omega_2(t')}{2}\sin\phi_1(t')dt'$$
$$=\int_0^t\left[\left[\frac{\partial}{\partial\xi}+\frac{1}{c}\frac{\partial}{\partial t'}\right]\frac{\Omega_2(t')}{2}\right]\sin\phi_1(t')dt'+\int_0^t\frac{\Omega_2(t')}{2}\left[\frac{\partial}{\partial\xi}+\frac{1}{c}\frac{\partial}{\partial t'}\right]\sin\phi_1(t')dt'$$
$$=\int_0^t-s_2\frac{\kappa_2}{2}\langle\sigma_{23}e^{-i\Delta' t'}\rangle_{\Delta'}\sin\phi_1(t')dt'+\int_0^t\frac{\Omega_2(t')}{2}\cos\phi_1(t')\left[\frac{\partial}{\partial\xi}+\frac{1}{c}\frac{\partial}{\partial t'}\right]\phi_1(t')dt'\ . \tag{B4}$$

We again will look at times $t\geq\xi$. Throughout this calculation, we will assume that we may perform the following approximate factorizations of integrals due to the small-overlap assumption:

$$\int_0^{\xi}f(\phi_2)h(\sin\phi_1,\cos\phi_1)dt'\simeq h(\sin\phi_1(\xi),\cos\phi_1(\xi))\int_0^{\xi}f(\phi_2)dt'\ .$$

We may then write

$$\int_0^{\xi}-s_2\frac{\kappa_2}{2}\langle\sigma_{23}e^{-i\Delta' t'}\rangle_{\Delta'}\sin\phi_1(t')dt'\simeq-s_2\frac{\kappa_2}{2}\sin\phi_1(\xi)\int_0^{\xi}\langle\sigma_{23}e^{-i\Delta' t'}\rangle_{\Delta'}dt'$$
$$\simeq-s_2\frac{\kappa_2}{2}\sin\phi_1(\xi)\pi g_{32}(0)\sigma_{23}(\xi,\Delta'=0)$$
$$\simeq-s_2\frac{\alpha_2}{4}\sin^3\phi_1(\xi)\sin[2\phi_2(\xi)] \tag{B5}$$

from Eqs. (7.17) and (7.19b). From Eqs. (7.16) and (7.19a) we obtain

$$\int_0^{\xi}\frac{\Omega_2(t')}{2}\cos\phi_1(t')\left[\frac{\partial}{\partial\tilde{z}}+\frac{1}{c}\frac{\partial}{\partial t'}\right]\phi_1(t')dt'$$

$$\simeq -s_1\frac{\alpha_1}{2}\int_0^{\xi}\frac{\Omega_2(t')}{2}\cos\phi_1(t')\sigma_{12}(t',\Delta=0)dt'$$

$$\simeq -s_1\frac{\alpha_1}{2}\int_0^{\xi}\frac{\Omega_2(t')}{2}\sin\phi_1(t')\cos^2\phi_1(t')\cos\phi_2(t')dt'$$

$$\simeq -s_1\frac{\alpha_1}{2}\int_0^{\xi}\left[\frac{\partial}{\partial t'}\phi_2(t')\sin\phi_1(t')\right]\cos^2\phi_1(t')\cos\phi_2(t')dt'$$

$$\simeq -s_1\frac{\alpha_1}{2}\sin\phi_1(\xi)\cos^2\phi_1(\xi)\int_0^{\xi}\cos\phi_2(t')\frac{\partial}{\partial t'}\phi_2(t')dt'\simeq -s_1\frac{\alpha_1}{2}\sin\phi_1(\xi)\cos^2\phi_1(\xi)\sin\phi_2(\xi)\ . \quad \text{(B6)}$$

Thus Eq. (B4) reduces to

$$\frac{\partial}{\partial z}[\phi_2(\Xi)\sin\phi_1(\Xi)]$$

$$\simeq\sin\phi_1(\Xi)\left[-s_2\frac{\alpha_2}{4}\sin^2\phi_1(\Xi)\sin[2\phi_2(\Xi)]\right.$$

$$\left.-s_1\frac{\alpha_1}{2}\cos^2\phi_1(\Xi)\sin\phi_2(\Xi)\right]\ , \quad \text{(B7)}$$

where we have transformed to the moving frame.

Using Eqs. (7.18) and (7.19) we may then summarize our results as follows.

Case I. We have

$$\frac{\partial}{\partial z}\phi_1\simeq -s_1\frac{\alpha_1}{4}\sin(2\phi_1)\ , \quad \text{(B8a)}$$

$$\frac{\partial}{\partial z}\phi_2\simeq -s_2\frac{\alpha_2}{4}\sin^2\phi_1\sin(2\phi_2)\ . \quad \text{(B8b)}$$

Case II. We have

$$\frac{\partial}{\partial z}\phi_1\simeq -s_1\frac{\alpha_1}{4}\sin(2\phi_1)\cos\phi_2\ , \quad \text{(B9a)}$$

$$\frac{\partial}{\partial z}(\phi_2\sin\phi_1)$$

$$\simeq\sin\phi_1\left[-s_2\frac{\alpha_2}{4}\sin^2\phi_1\sin(2\phi_2)-s_1\frac{\alpha_1}{2}\cos^2\phi_1\sin\phi_2\right]\ . \quad \text{(B9b)}$$

By rewriting these equations in terms of the areas defined by Eq. (4.7) we obtain Eqs. (7.20) and (7.21).

*Present address: Physics Department, University of Auckland, Private Bag, Auckland, New Zealand.

†Permanent address: Institute of Physics of the Polish Academy of Sciences, aleja Lotników 32/46 PL-02-668 Warsaw, Poland.

[1]F. T. Arecchi and R. Bonifacio, IEEE J. Quantum Electron. **QE-1**, 169 (1965).

[2]D. C. Burnham and R. Y. Chiao, Phys. Rev. **188**, 667 (1969).

[3]F. A. Hopf, P. Meystre, M. O. Scully, and J. F. Seely, Phys. Rev. Lett. **35**, 511 (1975).

[4]F. A. Hopf and P. Meystre, Phys. Rev. A **12**, 2534 (1975).

[5]F. A. Hopf, P. Meystre, and D. W. McLaughlin, Phys. Rev. A **13**, 777 (1976).

[6]N. E. Rehler and J. H. Eberly, Phys. Rev. A **3**, 1735 (1971).

[7]R. Bonifacio and L. A. Lugiato, Phys. Rev. A **11**, 1507 (1975); **12**, 587 (1975).

[8]J. C. MacGillivray and M. S. Feld, Phys. Rev. A **14**, 1169 (1976).

[9]F. A. Hopf and E. A. Overman II, Phys. Rev. A **19**, 1180 (1979).

[10]D. Polder, M. F. H. Schurmans, and Q. H. F. Vrehen, Phys. Rev. A **19**, 1192 (1979).

[11]F. Haake, H. King, G. Schröder, and J. Haus, Phys. Rev. A **20**, 2047 (1979).

[12]B. Sobolewska, B. J. Herman, P. D. Drummond, and J. H. Eberly, Opt. Lett. **6**, 408 (1981). Our definition of κ_j here corresponds to $2g_j$ in this earlier paper. The new definition is for compatibility with scaling used elsewhere. The unrationalized Gaussian unit formula is obtained by the replacement $\epsilon_0\rightarrow 1/4\pi$.

[13]J. N. Elgin and Li Fuli, Opt. Commun. **43**, 355 (1982).

[14]D. J. Kaup, Physica D **6D**, 143 (1983).

[15]H. Steudel, Physica D **6D**, 155 (1983).

[16]R. Meinel, Opt. Commun. **49**, 224 (1984).

[17]L. Allen and J. H. Eberly, *Optical Resonance and Two-Level Atoms* (Wiley, New York, 1975), p. 34.

[18]Reference 17, p. 41.

[19]F. J. Dyson, Phys. Rev. **75**, 486 (1949).

[20]R. M. Wilcox, J. Math. Phys. **8**, 962 (1967).

[21]We still must require that relation (3.8) holds in order for the approximation to be valid. This should cause no problem except at points where $\sin\phi_1(t)$ is near zero (i.e., $\phi_1\simeq\pm n\pi$). These points should be readily identifiable in the solution.

[22]We note that, in fact, owing to propagation, there is no cutoff time after which $\Omega_1(t)=0$. Nevertheless, $\Omega_1(t)$ is very small after a sufficient time interval, except for low-intensity ringing that does not transfer population in most cases. This is the region which we will identify as $\Omega_1(t)=0$. Numerical calculations given later in this paper will show that usually this ringing is negligible and the approximate expressions are very suitable for the calculation of optical pumping during propagation.

[23]Reference 17, p. 13.
[24]J. Rubenstein, J. Math. Phys. **11**, 258 (1970).
[25]M. J. Ablowitz, D. J. Kaup, A. C. Newell, and H. Segur, Phys. Rev. Lett. **30**, 1262 (1973).
[26]For applications to coherent pulses propagation, see D. J. Kaup, Phys. Rev. A **16**, 704 (1977), and references therein.
[27]P. D. Drummond (unpublished). See also P. D. Drummond and J. H. Eberly, Phys. Rev. A **25**, 3446 (1982).
[28]The exact distribution, which is valid for any value of N_J, is approximately Gaussian and will be given elsewhere.
[29]B. Sobolweska, Opt. Commun. **46**, 170 (1983).
[30]J. Mostowski and M. G. Raymer, Opt. Commun. **36**, 237 (1981).
[31]M. G. Raymer, K. Rzążewski, and J. Mostowski, Opt. Lett. **7**, 71 (1982).
[32]C. M. Bowden and C. C. Sung, Phys. Rev. Lett. **50**, 156 (1983).
[33]S. L. McCall and E. L. Hahn, Phys. Rev. **183**, 457 (1969); Phys. Rev. Lett. **18**, 908 (1967).
[34]W. Heitler, *The Quantum Theory of Radiation,* 3rd ed. (Oxford University, London, 1954), p. 69.
[35]We need not concern ourselves with the problem of $\phi_1 \simeq \pm n\pi$ stated in Ref. 21 since, for case I, the pulses are always well separated in time so that we need not make the small-overlap approximation to obtain Eqs. (7.18).